



Immune cells are increased in normal breast tissues of BRCA1/2 mutation carriers

Joshua Ogony¹ · Tanya L. Hoskin² · Melody Stallings-Mann³ · Stacey Winham² · Rushin Brahmabhatt⁴ · Muhammad Asad Arshad⁴ · Nagarajan Kannan⁶ · Alvaro Peña⁴ · Teresa Allers⁴ · Alyssa Brown⁵ · Mark E. Sherman¹ · Daniel W. Visscher⁶ · Keith L. Knutson⁷ · Derek C. Radisky³ · Amy C. Degnim⁴

Received: 15 June 2022 / Accepted: 25 October 2022 / Published online: 16 November 2022
© The Author(s), under exclusive licence to Springer Science+Business Media, LLC, part of Springer Nature 2022

Abstract

Purpose Breast cancer risk is elevated in pathogenic germline *BRCA 1/2* mutation carriers due to compromised DNA quality control. We hypothesized that if immunosurveillance promotes tumor suppression, then normal/benign breast lobules from BRCA carriers may demonstrate higher immune cell densities.

Methods We assessed immune cell composition in normal/benign breast lobules from age-matched women with progressively increased breast cancer risk, including (1) low risk: 19 women who donated normal breast tissue to the Komen Tissue Bank (KTB) at Indiana University Simon Cancer Center, (2) intermediate risk: 15 women with biopsy-identified benign breast disease (BBD), and (3) high risk: 19 prophylactic mastectomies from women with germline mutations in *BRCA1/2* genes. We performed immunohistochemical stains and analysis to quantitate immune cell densities from digital images in up to 10 representative lobules per sample. Median cell counts per mm² were compared between groups using Wilcoxon rank-sum tests.

Results Normal/benign breast lobules from *BRCA* carriers had significantly higher densities of immune cells/mm² compared to KTB normal donors (all $p < 0.001$): CD8+ 354.4 vs 150.9; CD4+ 116.3 vs 17.7; CD68+ 237.5 vs 57.8; and CD11c+ (3.5% vs 0.4% pixels positive). BBD tissues differed from BRCA carriers only in CD8+ cells but had higher densities of CD4+, CD11c+, and CD68+ immune cells compared to KTB donors.

Conclusions These preliminary analyses show that normal/benign breast lobules of *BRCA* mutation carriers contain increased immune cells compared with normal donor breast tissues, and BBD tissues appear overall more similar to BRCA carriers.

Keywords BRCA mutations · Benign breast disease · Breast lobule · Immune cells · Immune microenvironment

Introduction

Women with germline *BRCA1/2* mutations have substantially increased risk for breast cancer by age 70: 60% for *BRCA1* and 55% for *BRCA2* [1]. *BRCA* mutations lead to accumulation of DNA damage from double-strand DNA breaks due to inefficient homologous recombination DNA repair, leading to genomic instability and neoantigen generation [2–5]. *BRCA1* also regulates genomic stability via PLK1-driven cell division axis control, a mechanism defective in germline *BRCA1* mutation carriers [6, 7]. Compared to triple negative breast cancer (TNBCs) from *BRCA1*-wild-type patients, TNBCs with *BRCA1* mutation have elevated somatic mutation and tumor-infiltrating lymphocytes [8]. Similarly, *BRCA*-related breast cancer cases with germline and somatic *BRCA1/BRCA2* mutations have significantly

✉ Amy C. Degnim
degnim.amy@mayo.edu

¹ Quantitative Health Sciences, Mayo Clinic College of Medicine, Jacksonville, FL, USA

² Quantitative Health Sciences, Mayo Clinic College of Medicine, Rochester, MN, USA

³ Department of Cancer Biology, Mayo Clinic College of Medicine, Jacksonville, FL, USA

⁴ Department of Surgery, Mayo Clinic College of Medicine, 200 First St SW, Rochester, MN 55905, USA

⁵ Mayo Graduate School, Mayo Clinic, Rochester, MN, USA

⁶ Department of Laboratory Medicine and Pathology, Mayo Clinic, Rochester, MN, USA

⁷ Department of Immunology, Mayo Clinic, Jacksonville, USA

higher tumor mutational burden and neoantigen loads [9]. The accumulation of somatic mutations over time in normal breast tissue from germline *BRCA* mutation carriers may also lead to chronically higher neoantigen load, resulting in activation of the immune response, manifesting as increased immune cell infiltration. This group of women could potentially benefit from anti-inflammatory agents to lower breast cancer risk from low-grade chronic inflammation, or alternatively consider vaccine-related approaches that target abnormal epithelial cells.

In the breast, the immune system serves vital functions, including neonatal protection conveyed through breast milk, mammary gland protection from infection during lactation, and elimination of neoplastic epithelial cells through immunosurveillance [10–13]. The breast undergoes distinct histological changes during puberty, pregnancy, lactation, postpartum involution, and age-related lobular involution [14–16], and these changes are accompanied by immune cell composition alterations that may impact breast cancer risk [17–20]. We have characterized the immune microenvironment in normal breast tissues [21] and reported higher immune cell densities in breast tissues from women with benign breast disease (BBD) compared to normal research donors, suggesting overall increased inflammation associated with BBD, a condition of moderately increased breast cancer risk [22]. We also found that women with BBD who later developed breast cancer had significantly lower densities of CD20+ (B) cells, suggesting a possible link to immunosuppression associated with progression to cancer. These observations suggest that immune cell composition in breast tissue varies with risk, likely has a complex relationship with carcinogenesis, and may be especially relevant in *BRCA* carriers.

Here, we examine the breast tissue immune microenvironment in breast tissues with varying levels of breast cancer risk. We compared densities of major immune cell subsets: CD4+, CD8+ (T lymphocytes), CD11c+ (dendritic cells), CD20+ (B lymphocytes), and CD68+ (macrophages) in normal/benign breast lobules from high-risk germline *BRCA1/2* mutation carriers compared to age-matched women at intermediate breast cancer risk (BBD) or population-level breast cancer risk (KTB breast tissue donors).

Methods

Study population

Breast tissue samples in this study were obtained from women in three risk categories: (1) high risk (*BRCA1* or *BRCA2* mutation carriers), (2) intermediate risk (women from Mayo Clinic Benign Breast Disease (BBD) Cohort previously described [23], and (3) population risk (women

without clinical breast disease who donated breast tissue to the Susan G. Komen Foundation Tissue Bank (KTB) [24] for research purposes). BBD and KTB subjects were matched to *BRCA* mutation carriers on age at biopsy/surgery, thus creating matched “triplets.” The germline *BRCA* mutation subjects underwent surgery at Mayo Clinic between 1993 and 2012 and were either bilateral prophylactic mastectomy patients with no current or prior history of breast cancer in either breast or were contralateral prophylactic mastectomy patients in the setting of concurrent or prior breast cancer in the opposite breast. All prophylactic mastectomy specimens were confirmed negative for malignancy on final pathologic examination after surgery. For patients with bilateral prophylactic mastectomy, one breast was chosen randomly for this study. BBD samples were drawn from the Mayo Clinic BBD Cohort, which consists of more than 15,000 women who underwent surgical excision of a benign breast lesion at the Mayo Clinic in Rochester, Minnesota between January 1, 1967, and December 31, 2001. Study samples were randomly selected from the patients who underwent benign biopsies between 1992 and 2001 to make their acquisition timeframe more similar to both the *BRCA* and KTB samples. This study was approved by Mayo Clinic Institutional Review Board, and normal breast tissue collection from volunteer donors was approved by Institutional Review Board at Indiana University, Simon Cancer Center.

Tissue samples

The initial study set included 20 triplets from each category (*BRCA1/2*, $N=20$; BBD, $N=20$; KTB, $N=20$; total of 60 samples) for detailed immunostaining and immune cell quantitation. Serial sections were obtained from each sample for hematoxylin and eosin (H&E), and immunostains: T lymphocytes (CD4+, CD8+), dendritic cells (CD11c+), B lymphocytes (CD20+), and monocytes/macrophages (CD68+). Matched samples (*BRCA1/2*, BBD, and KTB) were immunostained within the same batch to minimize the batch effects that could affect comparison of immune cell densities across groups. The final sample set used for analysis included 53 tissue samples (*BRCA1/2*, $N=19$; BBD, $N=15$; KTB, $N=19$) due to damaged lobules or lack of intact lobules in 7 samples.

Immunohistochemical staining

Formalin-fixed paraffin embedded tissue sections were processed as previously described [25], followed by immunohistochemical staining as follows: CD4 (Leica Novocastra NCL-CD4-368-L-CE at 1:50), CD8 (DAKO M7103 at 1:20), CD11c (Leica Novocastra NCL-L-CD11c-563 at

1:25), CD20 (DAKO M0755 at 1:60), CD45 (DAKO M0710 at 1:1,500), and CD68 (DAKO, M0876 at 1:100).

Digitization of slides and histologic lobule annotation

ScanScope XT slide scanner (Aperio Technologies) was used to capture whole slide digital images of breast tissue samples at 20X objective, followed by analysis using Aperio ImageScope software (<http://www.aperio.com/pathology-services/imagescope-slide-viewing-software.asp>). The study pathologist assessed the digital H&E images to select and annotate up to 10 representative lobules, which were circled and numerically labeled from 1 to 10. The same lobules selected on the H&E digital images were identified on each immunostained digital image, circled, and assigned the corresponding lobule number. Immune cells were quantified

from the digital images using Spectrum version 11 using an FDA-approved algorithm within ImageScope.

Digital image analysis

The procedure for counting positively stained immune cells from digital images of immunohistochemically stained tissues sections has been previously described [21]. Briefly, an optimized FDA-approved algorithm was applied uniformly to all circled lobules for a particular immunostain for all samples. The positively stained cells were recorded on a per lobule basis as density (cells/mm²) for CD4+, CD8+, CD20+, and CD68+ cells in each sample, but for CD11c+, positive to total pixel ratio was assessed to quantitate positive cells due to diffuse staining (Fig. 1). The data output from image analysis in Aperio ImageScope was exported into a data file, and densities of each immune cell subtype

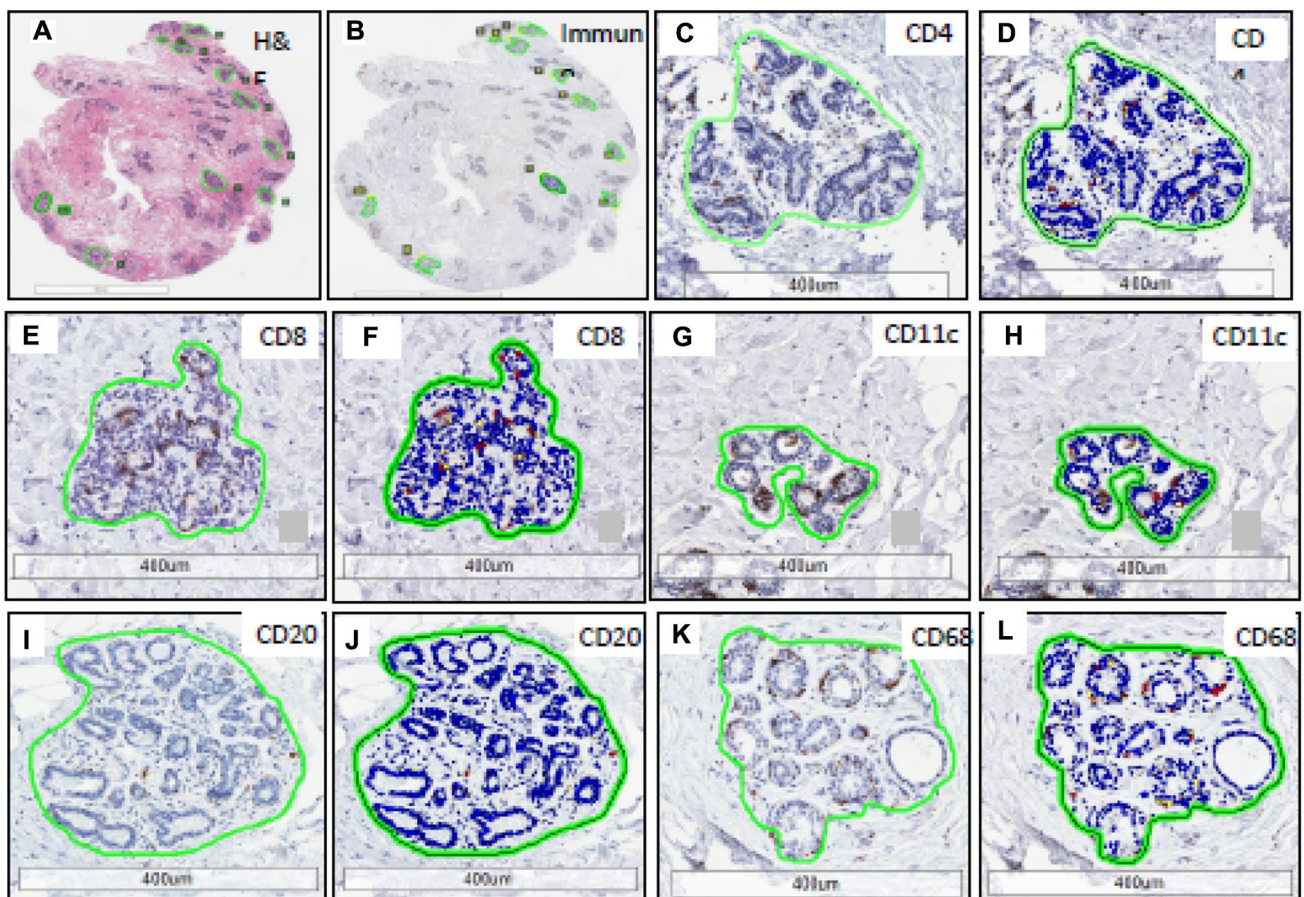


Fig. 1 Analysis of immune cell subtypes in digital images of breast tissue of women at varying degrees of risk. **A** H&E image from a tissue sample of one of the patients included in the study, with representative lobules circled by the study pathologist. **B** immunostained section of tissue from the same sample as (**A**), with the same lobules as labeled in (**A**) identified and circled and tissue appearance annotated. **C** CD4+staining of a lobule. **D** analysis of CD4+stain-

ing of lobule in (**C**). **E** CD8+staining of a lobule. **F** analysis of CD8+staining of lobule in (**E**). **G** CD11c+staining of a lobule. **H** Analysis of CD11c+staining of lobule in (**G**). **I** CD20+staining of a lobule. **J** Analysis of CD20+staining of lobule in (**I**). **K** CD68+staining of a lobule. **L** Analysis of CD68+staining of lobule in (**K**)

were calculated as cells/mm² (or percent of pixels positive for CD11c+ cells) for each lobule. We evaluated immune cell densities in the lobules because we and others have previously shown that immune cells are predominantly localized to lobules rather than stroma [21, 26].

Statistical analysis

The median immune cell density across all lobules within a given sample was calculated and used for a per-subject analysis. Groups were compared using Wilcoxon rank-sum tests for univariate analysis. Multivariable analysis was performed using logistic regression models for pairwise comparisons between groups, adjusted for age and the percent of annotated lobules that were fibrocystic for each sample. The Firth penalized likelihood bias reduction method and profile-likelihood confidence intervals were utilized to improve performance with sparse data [27]. Immune cell measures were transformed using a Van Der Waerden normalizing transformation for logistic regression modeling and for visualization with a heatmap. Analysis was performed using SAS (SAS Institute Inc., version 9.4) and R software (<https://www.r-project.org/>). $p < 0.05$ was considered statistically significant.

Results

Study population and tissue samples

After excluding samples without benign evaluable lobules, the final study set included 19 *BRCA* carriers, 15 women with BBD, and 19 KTB donors. Among the 19 germline *BRCA* mutation carriers, 9 were *BRCA1* and 10 were *BRCA2*. In the 15 BBD subjects included in the final analysis, 7 had nonproliferative BBD and 8 had proliferative disease without atypia. Median age in the final sample set was 44 years (range 34–67 years), with 51% age < 45 years, 32% age 45–55 years, and 17% age > 55. Groups remained well matched for age in the final sample set, with median age 43 years (range 34–67) among *BRCA* carriers, 45 years (range 34–67) among women with BBD, and 44 years (range 34–67) among KTB donors (Table 1). The median lifetime Breast Cancer Risk Assessment Tool (<https://bcrisktool.cancer.gov/>) risk score was 11.7% (range 6.1–22.3%) in BBD subjects and 10.3% (range 6.9–19.0%) in KTB subjects, $p = 0.28$. Fewer than half of the BBD (46.2%) and KTB (43.8%) subjects had family history of blood relatives with breast and/or ovarian cancer, compared to 100% of the *BRCA* subjects. *BRCA* mutation carriers and BBD patients had a higher percentage of fibrocystic lobules (median 50% fibrocystic lobules and 50% normal lobules in both *BRCA*

and BBD groups) as compared with KTB samples (median 20% fibrocystic lobules and 80% normal lobules), $p < 0.001$.

Immune cell densities vary across tissue groups of varying risk

Overall trends

Positive staining for immune cell subtypes CD4+, CD8+, CD11c, and CD68+ was found for a large majority of samples (87–100% of samples had a non-zero within-sample median across lobules); CD20 staining was low with 42.3% of the samples overall having a within-sample median CD20 of zero, including 44.4% of *BRCA* samples, 26.7% of BBD samples, and 52.6% of KTB samples (Table 2 and Fig. 2). CD8+ cell density decreased with decreasing risk categories, with highest density in *BRCA* mutation samples: 354.4 cells/mm² in *BRCA* samples, 200.0 cells/mm² in BBD samples, and 150.9 cells/mm² in KTB. A similar pattern was observed across risk categories for CD4+ cells. Dendritic cells (CD11c+) were quantified as percent of pixels that were positive and had similar abundance in *BRCA* mutation and BBD samples (median 3.5% and 3.4% pixels positive, respectively), with significantly lower density in KTB samples (median 0.4% pixels positive, $p < 0.001$ compared to *BRCA*). Macrophages (CD68+) were also similar in *BRCA* and BBD samples (median 237.5 vs 219 cells/mm², respectively) but markedly lower in KTB samples (median 57.8 cells/mm², $p < 0.001$ compared to *BRCA*). CD20+ cells were low in all groups and not statistically different across the three groups ($p = 0.08$).

BRCA samples versus other groups

The majority of the immune cell subtypes (CD4, CD8, CD11c, and CD68) had higher densities in the high-risk *BRCA* mutation samples, and these differences were statistically significant in pairwise comparisons with KTB samples (each $p < 0.001$), whereas in comparison with BBD samples, only CD8+ cells were higher in *BRCA* samples.

BBD samples versus other groups

Immune cell densities in BBD samples were generally similar to *BRCA* samples except for CD8+ cells, which were significantly lower in BBD samples ($p = 0.01$). BBD samples differed significantly from KTB samples with respect to CD4+, CD11c+, and CD68+ cells and were overall more similar to the *BRCA* samples. The heatmap in Fig. 3 shows that while the *BRCA* and KTB samples are mostly distinct, the BBD samples' immune cell patterns are variable but more often group with the *BRCA* samples (only 3 BBD samples grouped with the KTB samples).

Table 1 Characteristics of subjects included in the study by risk category

	BRCA N=19	BBD N=15	KTB N=19	BRCA vs BBD p-value	BRCA vs KTB p-value	BBD vs KTB p-value
Age, years, median (IQR)	43 (39–50)	45 (39–54)	44 (40–50)	0.82	0.80	0.99
Age category, n (%)				> 0.99	> 0.99	> 0.99
<45	10 (52.6%)	7 (46.7%)	10 (52.6%)			
45–55	6 (31.6%)	5 (33.3%)	6 (31.6%)			
> 55	3 (15.8%)	3 (20.0%)	3 (15.8%)			
Menopausal status, n (%)				0.72	0.82	> 0.99
Pre-menopausal	12 (63.2%)	9 (69.2%)	12 (66.7%)			
Post-menopausal	7 (36.8%)	4 (30.8%)	6 (33.3%)			
Unknown	0	2	1			
Race, n (%)				0.71	0.73	0.45
American Indian	0	1 (6.7%)	0			
Asian	1 (5.3%)	1 (6.7%)	0			
Black	0	0	1 (5.9%)			
White	18 (94.7%)	13 (86.7%)	16 (94.1%)			
Other/Unknown	0	0	2			
Family history of blood relatives with breast or ovarian cancer, n (%)				<0.001	<0.001	> 0.99
Yes	19 (100%)	6 (46.2%)	7 (43.8%)			
No	0	7 (53.8%)	9 (56.3%)			
Unknown	0	2	3			
Parity, n (%)				> 0.99	0.66	0.63
Nulliparous	2 (10.5%)	1 (8.3%)	3 (16.7%)			
Parous	17 (89.5%)	11 (91.7%)	15 (83.3%)			
Unknown	0	3	1			
BMI, median (IQR)	26.0 (21.8–28.6)	24.0 (23.0–28.0)	29.8 (24.0–33.4)	0.94	0.05	0.06
Percent of annotated lobules fibro- cystic, median (IQR)	50 (30–60)	50 (40–70)	20 (0–38)	0.30	p < 0.001	p < 0.001

IQR interquartile range, pp pixel positive

Table 2 Pairwise Wilcoxon rank-sum p-values comparing median immune cell densities in breast lobules from women with BRCA germline mutations, vs BBD and KTB groups

All Lobules	BRCA Median (IQR)	BBD Median (IQR)	KTB Median (IQR)	BRCA vs BBD p-value	BRCA vs KTB p-value	BBD vs KTB p-value
CD4+, cells/mm ²	116.3 (46.4–183.6)	63.8 (25.0–121.1)	17.7 (13.3–40.6)	0.08	< 0.001	0.01
CD8+, cells/mm ²	354.4 (285.5–473.2)	200 (118.9–385)	150.9 (110.1–225.0)	0.01	< 0.001	0.30
CD11c+, % pp	3.5 (1.9–6.8)	3.4 (1.6–4.7)	0.4 (0–0.6)	0.68	< 0.001	< 0.001
CD20+, cells/mm ²	6.2 (0–25.4)	16.7 (0–58.3)	0 (0–20.8)	0.16	0.66	0.07
CD68, cells/mm ²	237.5 (122.9–281.8)	219 (75.0–459.4)	57.8 (29.2–100.0)	> 0.99	< 0.001	0.002

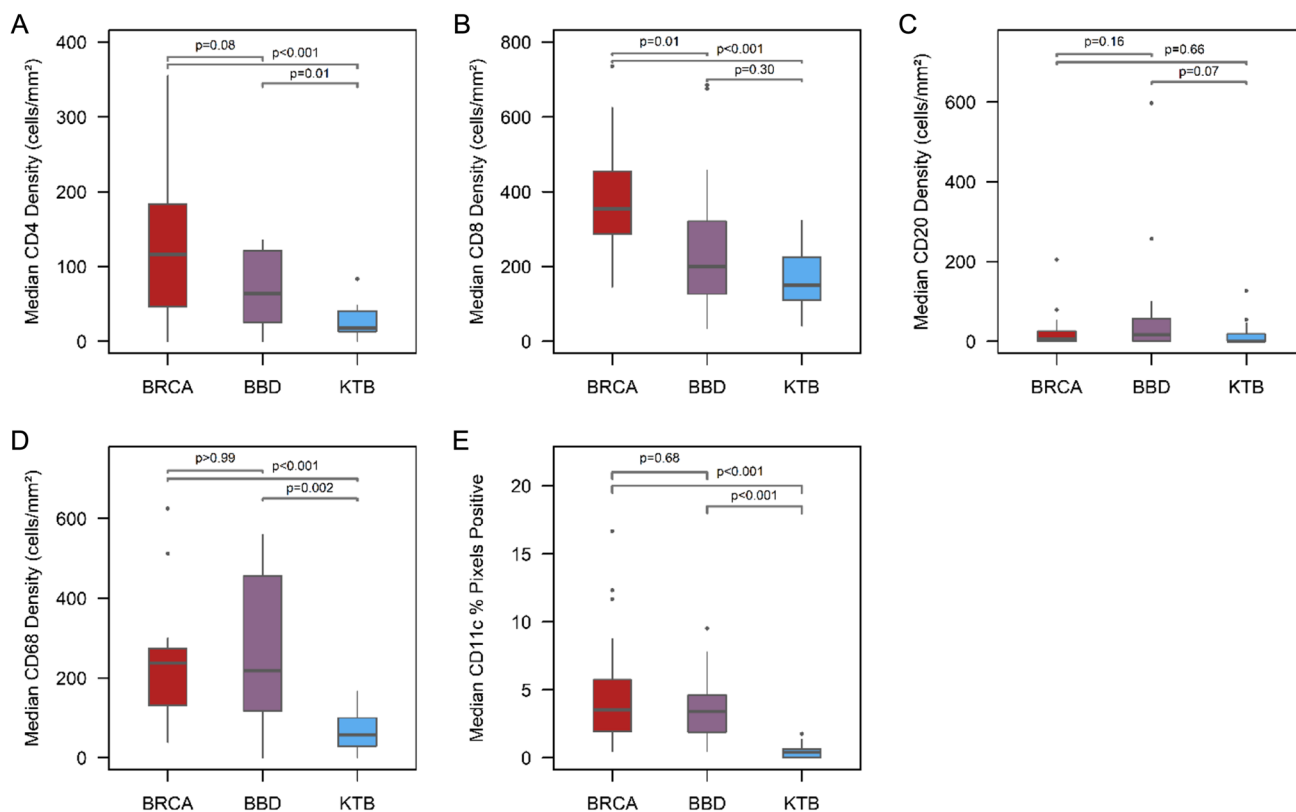


Fig. 2 Median densities of immune cells measured in all lobules in at-risk breast tissue (BRCA 1/2, BBD, KTB). **A** CD4+, **B** CD8+, **C** CD20+, **D** CD68+ immune cell densities (cells/mm²), **E** CD11c percent of pixels positive. *p*-values for pairwise comparisons between groups are annotated for each immune cell type. BRCA samples showed significantly higher densities than KTB samples for every

immune cell type except CD20+ cells, but BRCA samples showed no significant difference from BBD samples for any immune cell type except CD8+ cells. BBD samples showed significantly higher densities of CD4+, CD68+, and CD11c+ cells as compared to KTB samples.

Multivariable analysis

We performed multivariable logistic regression to assess the differences between groups adjusted for age because it was an initial matching variable and for percent of fibrocystic lobules as a potential confounding variable that was significantly lower in KTB samples. The multivariable models confirmed the univariate analysis findings for comparisons between all three groups (Supplemental Table 1).

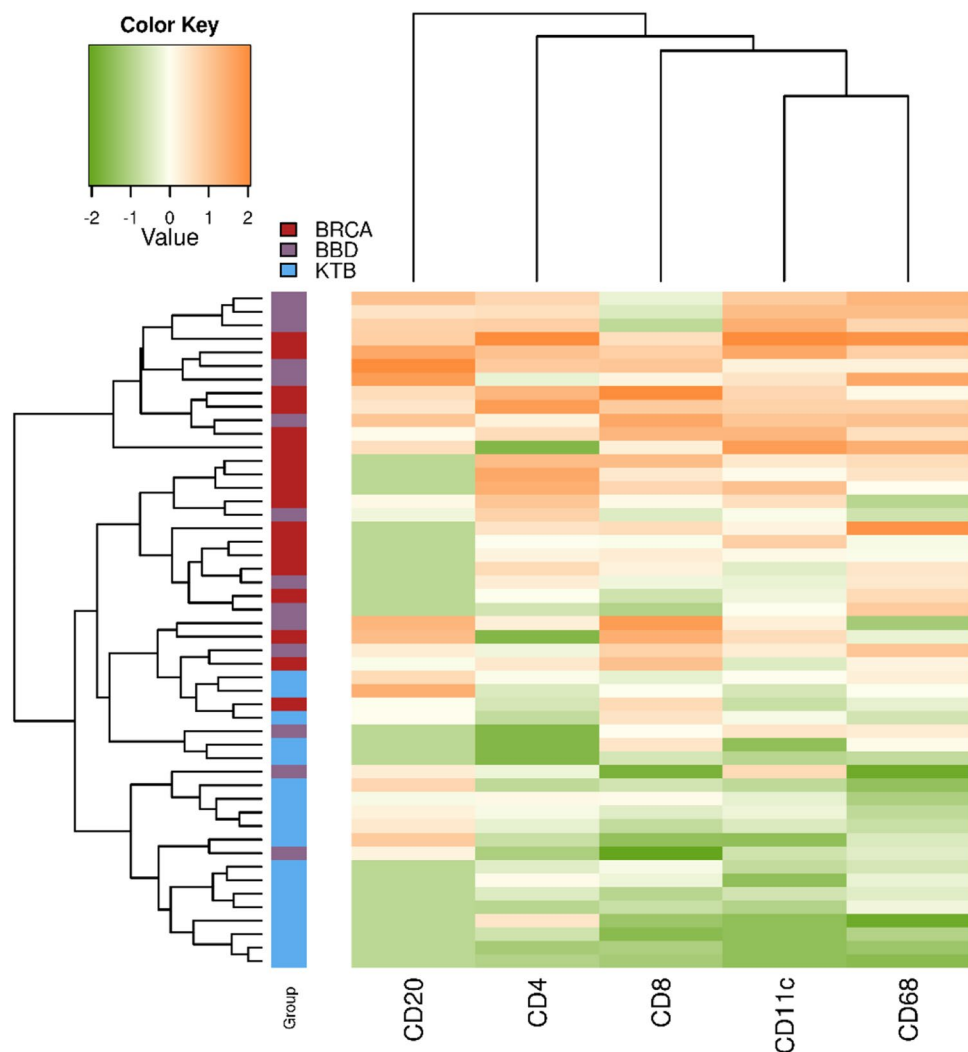
Discussion

In this investigation, we found that densities of T lymphocytes (CD4+, CD8+), dendritic cells (CD11c+), and macrophages (CD68+) were significantly higher in germline *BRCA1/2* mutation carrier samples compared to breast tissue samples from normal donors, suggesting increased cell-mediated immunity in breast tissues from women at high risk due to germline *BRCA* mutations. These findings are relevant, as the role of the immune microenvironment

in carcinogenesis remains unclear, and investigation into mammary epithelium experiencing genomic instability events due to germline *BRCA1/2* mutation affords a window into normal-appearing breast tissues with high future breast cancer risk. Although the immune cell presence in breast tissue from *BRCA1/2* mutation carriers appeared more similar overall to BBD women than KTB normal tissue donors, the *BRCA1/2* carriers still showed significantly higher CD8+ cell densities compared to women with BBD. Taken together, these findings suggest that in breast tissues from *BRCA* mutation carriers, the immune cell presence is significantly greater than that of breast tissue at normal/population risk and also enriched for CD8+ cells compared to BBD tissues.

Immune infiltrates on H&E have been reported in morphologically normal breast lobules in 51% of women undergoing prophylactic mastectomy due to hereditary high risk, compared with 10% of reduction mammoplasty tissues [28]. A separate study of immune infiltrates in background normal tissues of 334 breast cancer patients demonstrated association with clinicopathologic features more commonly seen

Fig. 3 Heatmap of normal-transformed densities across the immune cell subtypes in BRCA, BBD, and KTB samples. BRCA (red group) and KTB (blue group) samples are almost completely distinct (only 1 BRCA sample groups with the KTB samples), and BBD samples appear more similar to BRCA samples (only 3 BBD samples group with KTB samples). The general pattern was for BRCA samples (and most BBD samples) to have relatively consistent higher densities (orange shade) of CD4+, CD8+, CD11c+, and CD68+ cells, whereas KTB samples had consistently lower densities (green shade) of these four immune cell types. Results were more mixed for CD20+ cells without a clear pattern of higher/lower expression across the three study groups



in hereditary breast cancer (younger age, triple negative, and medullary phenotypes) [29]. Hussein et al. described increasing densities of B cells, macrophages, and cytotoxic T cells across the spectrum of concurrent normal/benign abnormality/DCIS/invasive cancer areas in mastectomy specimens, but BRCA mutation status was unknown in these patients [30]. Similarly, Ruffell et al. described immune cell subpopulations in small numbers of paired normal and breast tumor tissues (also with unknown BRCA status) and reported increases in CD4+ cells in tumor tissues, contrasted with increased macrophage presence in normal tissues [31]. However, data are lacking that compare immune content of normal/benign breast lobules from mutation carriers to women without known mutations.

Previously, we have characterized the immune cell landscape in BBD samples and in normal donor breast tissues, showing that CD8+ T lymphocytes, CD20+ B lymphocytes, and dendritic cells (CD11c) are present at higher densities in BBD samples compared with normal donor tissues [22]. In the present study, we expanded this work to *BRCA1/2*

mutation carriers, observing that immune cell densities are also significantly higher in *BRCA1/2* mutation carriers versus normal donor tissues, suggesting activated immune response. It remains to be determined whether the increase in immune cell densities in *BRCA1/2* mutation carriers represents tumor-suppressive immunosurveillance induced by alterations in epithelium, or rather tumor-promoting chronic inflammation.

Why would there be increased T cell responses in breast lobules from *BRCA* mutation carriers compared to normal women of similar age? Previous studies have shown that *BRCA* mutations result in deficient DNA damage repair by homologous recombination, leading to increased tumor mutational burden [32] that can result in the formation of neoantigens that may be recognized as foreign targets by the immune system [33]. Increased mutation/neoantigen load in breast cancer has been associated with increased cancer-specific tumor-infiltrating lymphocytes (TILs) [34, 35], and increasing neoantigen load from single-nucleotide mutations and INDELS was associated with better overall survival in primary breast tumors from the Cancer Genome

Atlas [9]. In addition to increasing the load of immunogenic neoantigens, *BRCA* mutations may also modulate immunity in other ways. For example, *BRCA* mutations are also known to increase autophagy which has been linked to the generation of antigenic peptides presented in MHC class I and class II molecules [36]. Similarly, *BRCA* mutation results in genetic instability and susceptibility to apoptosis which may result in release of danger signals and antigens into the tissue environment which could explain increased DC infiltration and subsequent T cell expansion [37].

Our finding that the densities of macrophages were significantly higher in both germline *BRCA* mutation carriers and BBD samples as compared with normal KTB tissue samples may suggest chronic inflammation; however, these results need to be interpreted with caution since by virtue of their plasticity, macrophages may also exert anti-inflammatory effects (i.e., M2 macrophages), depending on microenvironmental context. Macrophages can express pro-inflammatory cytokines such as IFN- γ , TNF- α , IL-1 β , and IL-6 that promote chronic inflammation and tissue injury, resulting in increased risk of tumor development [38, 39]. Macrophages assume a continuum of activation states in their adaptive responses, ranging from M1 polarization to M2 polarization states, and the specific role, whether M2 polarized (immunosuppressive) or M1 polarized (pro-inflammatory) may depend on the cytokine milieu of the tissue microenvironment [40]. In a study of single cell sequencing in 8 paired breast cancers and normal breast tissue, Azizi et al. reported findings that support a model of continuous T cell activation intertwined with both M1 and M2 macrophage phenotypes, an observation that contrasts with the M2 macrophage polarization model of cancer which is immune suppressive [41]. While these findings support the idea that the increased immunity we observed in the present study is a chronic inflammatory response, this remains an area for further study. These future studies could include a more detailed analysis of the infiltrating T cells addressing whether they are differentiated effector T cells (e.g., cytotoxic, Th1, Th2, or Th17) or immunosuppressive regulatory T cells.

The strengths of our study include the novel finding of increased CD4+ and CD8+ T lymphocytes, CD68+ macrophages, and CD11c+ dendritic cells in *BRCA* germline mutation carriers, and the detailed quantification across multiple lobules per sample. The primary limitation of our study, however, is a small sample size. Despite this, several significant differences were identified due to the large magnitude of differences between the *BRCA* and KTB samples. Selection bias regarding lobules studied is another limitation. Whereas our study was limited to quantitating major immune cell subtypes, rather than specific phenotypes (for example, CD8+ cells as cytotoxic T cells or regulatory T cells, CD4+ T cells as Th1, Th2, Th17, and macrophage phenotypes), it provides a background for our future studies in which we could

use NanoString DSP to understand epithelial status versus immune cells, combined with spatial RNA sequencing to visualize the effects of altered epithelium together with loss of *BRCA* function and how this correlates with immune response.

In conclusion, we have demonstrated the novel finding that immune cell quantities of T lymphocytes (CD4+, CD8+), dendritic cells, and macrophages (CD68+) are significantly higher in breast tissue lobules from *BRCA* mutation carrier normal/benign samples as compared to normal donor tissue samples (KTB). BBD tissues appear more similar to *BRCA* carriers, consistent with increased risk status. Possible association of neoantigen load with specific immune infiltrates and more detailed approaches for immune subtyping are areas of investigation that will help to elucidate better the role of the immune system in breast carcinogenesis in high-risk women.

Supplementary Information The online version contains supplementary material available at <https://doi.org/10.1007/s10549-022-06786-y>.

Acknowledgements We acknowledge the funding from the Mayo Clinic Department of Surgery and Mayo Clinic Breast SPORE through a Developmental Research Project awarded to Dr. Mark Sherman in support of this project. Data from the Susan G. Komen Tissue Bank at the IU Simon Cancer Center were used in this study. We thank contributors, including Indiana University who collected data used in this study, as well as donors and their families, whose help and participation made this work possible.

Funding The funded was provided by National Cancer Institute (Grant No. P50CA116201).

Data availability The datasets generated during and/or analysed during the current study are available from the corresponding author on reasonable request.

References

1. Mavaddat N, Peock S, Frost D, Ellis S, Platte R, Fineberg E et al (2013) Cancer risks for *BRCA1* and *BRCA2* mutation carriers: results from prospective analysis of EMBRACE. *J Natl Cancer Inst* 105(11):812–822
2. Gudmundsdottir K, Ashworth A (2006) The roles of *BRCA1* and *BRCA2* and associated proteins in the maintenance of genomic stability. *Oncogene* 25(43):5864–5874
3. Venkitaraman AR (2001) Functions of *BRCA1* and *BRCA2* in the biological response to DNA damage. *J Cell Sci* 114(Pt 20):3591–3598
4. Strickland KC, Howitt BE, Shukla SA, Rodig S, Ritterhouse LL, Liu JF et al (2016) Association and prognostic significance of *BRCA1/2*-mutation status with neoantigen load, number of tumor-infiltrating lymphocytes and expression of PD-1/PD-L1 in high grade serous ovarian cancer. *Oncotarget* 7(12):13587–13598
5. Nolan E, Vaillant F, Branstetter D, Pal B, Giner G, Whitehead L et al (2016) RANK ligand as a potential target for breast cancer prevention in *BRCA1*-mutation carriers. *Nat Med* 22(8):933–939
6. He Z, Ghorayeb R, Tan S, Chen K, Lorentzian AC, Bottyan J et al (2022) Pathogenic *BRCA1* variants disrupt PLK1-regulation of mitotic spindle orientation. *Nat Commun* 13(1):2200

7. He Z, Kannan N, Nemirovsky O, Chen H, Connell M, Taylor B et al (2017) BRCA1 controls the cell division axis and governs ploidy and phenotype in human mammary cells. *Oncotarget* 8(20):32461–32475
8. Nolan E, Savas P, Policheni AN, Darcy PK, Vaillant F, Mintoff CP et al (2017) Combined immune checkpoint blockade as a therapeutic strategy for BRCA1-mutated breast cancer. *Sci Transl Med*. <https://doi.org/10.1126/scitranslmed.aal4922>
9. Ren Y, Cherukuri Y, Wickland DP, Sarangi V, Tian S, Carter JM et al (2020) HLA class-I and class-II restricted neoantigen loads predict overall survival in breast cancer. *Oncoimmunology* 9(1):1744947
10. Brandtzaeg P (2010) The mucosal immune system and its integration with the mammary glands. *J Pediatr* 156(2 Suppl):S8–15
11. Goldman AS (1993) The immune system of human milk: antimicrobial, antiinflammatory and immunomodulating properties. *Pediatr Infect Dis J* 12(8):664–671
12. Spencer JP (2008) Management of mastitis in breastfeeding women. *Am Fam Phys* 78(6):727–731
13. Zumwalde NA, Haag JD, Sharma D, Mirrieles JA, Wilke LG, Gould MN et al (2016) Analysis of immune cells from human mammary ductal epithelial organoids reveals Vδ2+ T cells that efficiently target breast carcinoma cells in the presence of bisphosphonate. *Cancer Prev Res (Phila)* 9(4):305–316
14. Hebbard L, Steffen A, Zawadzki V, Fieber C, Howells N, Moll J et al (2000) CD44 expression and regulation during mammary gland development and function. *J Cell Sci* 113(Pt 14):2619–2630
15. Gillespie SL, Porter K, Christian LM (2016) Adaptation of the inflammatory immune response across pregnancy and postpartum in Black and White women. *J Reprod Immunol* 114:27–31
16. O'Brien J, Lyons T, Monks J, Lucia MS, Wilson RS, Hines L et al (2010) Alternatively activated macrophages and collagen remodeling characterize the postpartum involuting mammary gland across species. *Am J Pathol* 176(3):1241–1255
17. Schedin P, O'Brien J, Rudolph M, Stein T, Borges V (2007) Microenvironment of the involuting mammary gland mediates mammary cancer progression. *J Mammary Gland Biol Neoplasia* 12(1):71–82
18. McDaniel SM, Rumer KK, Biroc SL, Metz RP, Singh M, Porter W et al (2006) Remodeling of the mammary microenvironment after lactation promotes breast tumor cell metastasis. *Am J Pathol* 168(2):608–620
19. Lyons TR, O'Brien J, Borges VF, Conklin MW, Keely PJ, Eliceiri KW et al (2011) Postpartum mammary gland involution drives progression of ductal carcinoma in situ through collagen and COX-2. *Nat Med* 17(9):1109–1115
20. Milanese TR, Hartmann LC, Sellers TA, Frost MH, Vierkant RA, Maloney SD et al (2006) Age-related lobular involution and risk of breast cancer. *J Natl Cancer Inst* 98(22):1600–1607
21. Degnim AC, Brahmabhatt RD, Radisky DC, Hoskin TL, Stallings-Mann M, Laudenschlager M et al (2014) Immune cell quantitation in normal breast tissue lobules with and without lobulitis. *Breast Cancer Res Treat* 144(3):539–549
22. Degnim AC, Hoskin TL, Arshad M, Frost MH, Winham SJ, Brahmabhatt RA et al (2017) Alterations in the immune cell composition in premalignant breast tissue that precede breast cancer development. *Clin Cancer Res* 23(14):3945–3952
23. Hartmann LC, Sellers TA, Frost MH, Lingle WL, Degnim AC, Ghosh K et al (2005) Benign breast disease and the risk of breast cancer. *New Engl J Med* 353(3):229–237
24. Sherman ME, Figueroa JD, Henry JE, Clare SE, Rufenbarger C, Storniolo AM (2012) The Susan G. Komen for the Cure Tissue Bank at the IU Simon Cancer Center: a unique resource for defining the “molecular histology” of the breast. *Cancer Prev Res (Phila)* 5(4):528–535
25. Radisky DC, Santisteban M, Berman HK, Gauthier ML, Frost MH, Reynolds CA et al (2011) p16(INK4a) expression and breast cancer risk in women with atypical hyperplasia. *Cancer Prev Res (Phila)* 4(12):1953–1960
26. Zirbes A, Joseph J, Lopez JC, Sayaman RW, Basam M, Seewaldt VL et al (2021) Changes in immune cell types with age in breast are consistent with a decline in immune surveillance and increased immunosuppression. *J Mammary Gland Biol Neoplasia* 26(3):247–261
27. Heinze G, Pühr R (2010) Bias-reduced and separation-proof conditional logistic regression with small or sparse data sets. *Stat Med* 29(7–8):770–777
28. Hermsen BB, von Mensdorff-Pouilly S, Fabry HF, Winters HA, Kenemans P, Verheijen RH et al (2005) Lobulitis is a frequent finding in prophylactically removed breast tissue from women at hereditary high risk of breast cancer. *J Pathol* 206(2):220–223
29. Gulbahce HE, Vanderwerf S, Blair C, Sweeney C (2014) Lobulitis in nonneoplastic breast tissue from breast cancer patients: association with phenotypes that are common in hereditary breast cancer. *Hum Pathol* 45(1):78–84
30. Hussein MR, Hassan HI (2006) Analysis of the mononuclear inflammatory cell infiltrate in the normal breast, benign proliferative breast disease, in situ and infiltrating ductal breast carcinomas: preliminary observations. *J Clin Pathol* 59(9):972–977
31. Ruffell B, Au A, Rugo HS, Esserman LJ, Hwang ES, Coussens LM (2012) Leukocyte composition of human breast cancer. *Proc Natl Acad Sci USA* 109(8):2796–2801
32. Wen WX, Leong CO (2019) Association of BRCA1- and BRCA2-deficiency with mutation burden, expression of PD-L1/PD-1, immune infiltrates, and T cell-inflamed signature in breast cancer. *PLoS ONE* 14(4):e0215381
33. Castle JC, Uduman M, Pabla S, Stein RB, Buell JS (2019) Mutation-derived neoantigens for cancer immunotherapy. *Front Immunol* 10:1856
34. Luen S, Virassamy B, Savas P, Salgado R, Loi S (2016) The genomic landscape of breast cancer and its interaction with host immunity. *Breast (Edin)* 29:241–250
35. Kato T, Park JH, Kiyotani K, Ikeda Y, Miyoshi Y, Nakamura Y (2017) Integrated analysis of somatic mutations and immune microenvironment of multiple regions in breast cancers. *Oncotarget* 8(37):62029–62038
36. Morand S, Stanbery L, Walter A, Rocconi RP, Nemunaitis J (2020) BRCA1/2 Mutation Status Impact on Autophagy and Immune Response: Unheralded Target. *JNCI Cancer Spectr* 4(6):pkaa077
37. Reisländer T, Lombardi EP, Groelly FJ, Miar A, Porru M, Di Vito S et al (2019) BRCA2 abrogation triggers innate immune responses potentiated by treatment with PARP inhibitors. *Nat Commun* 10(1):3143
38. Oishi Y, Manabe I (2018) Macrophages in inflammation, repair and regeneration. *Int Immunol* 30(11):511–528
39. Hamidzadeh K, Christensen SM, Dalby E, Chandrasekaran P, Mosser DM (2017) Macrophages and the recovery from acute and chronic inflammation. *Annu Rev Physiol* 79:567–592
40. Locati M, Curtale G, Mantovani A (2020) Diversity, mechanisms, and significance of macrophage plasticity. *Annu Rev Pathol* 15:123–147
41. Azizi E, Carr AJ, Plitas G, Cornish AE, Konopacki C, Prabhakaran S et al (2018) Single-cell map of diverse immune phenotypes in the breast tumor microenvironment. *Cell* 174(5):1293–1308.e36

Publisher's Note Springer Nature remains neutral with regard to jurisdictional claims in published maps and institutional affiliations.

Springer Nature or its licensor (e.g. a society or other partner) holds exclusive rights to this article under a publishing agreement with the author(s) or other rightsholder(s); author self-archiving of the accepted manuscript version of this article is solely governed by the terms of such publishing agreement and applicable law.